Basal forebrain atrophy along the Alzheimer's disease spectrum and its relevance for subjective cognitive decline

Shumei Li
German Center for Neurodegenerative Diseases, Bonn
Michel J. Grothe
German Center for Neurodegenerative Diseases, Rostock
Marcel Daamen
German Center for Neurodegenerative Diseases, Rostock
Steffen Wolfsgruber
German Center for Neurodegenerative Diseases, Bonn
Frederic Brosseron
German Center for Neurodegenerative Diseases, Bonn
Katharina Buerger
German Center for Neurodegenerative Diseases, Munich
Cihan Catak
Ludwig Maximilian University of Munich
Laura Dobisch
German Center for Neurodegenerative Diseases, Magdburg
Enise Irem Incesoy
German Center for Neurodegenerative Diseases, Berlin
Klaus Fliessbach
German Center for Neurodegenerative Diseases, Bonn
Christiana Franke
Charite, Berlin
Michael T. Heneka
German Center for Neurodegenerative Diseases, Bonn
Ingo Kilimann
German Center for Neurodegenerative Diseases, Rostock
Luca Kleineidam
German Center for Neurodegenerative Diseases, Bonn
Christoph Laske
German Center for Neurodegenerative Diseases, Tubingen
Coraline D. Metzger

German Center for Neurodegenerative Diseases, Magdeburg
Matthias Munk
German Center for Neurodegenerative Diseases, Tubingen
Oliver Peters
German Center for Neurodegenerative Diseases, Berlin
Lukas Preis
German Center for Neurodegenerative Diseases, Berlin
Josef Priller
German Center for Neurodegenerative Diseases, Berlin
Alfredo Ramirez
University of Cologne
Anja Schneider
German Center for Neurodegenerative Diseases, Bonn
Annika Spottke
German Center for Neurodegenerative Diseases, Bonn
Björn H. Schott
German Center for Neurodegenerative Diseases, Gottingen
Eike Jakob Spruth
German Center for Neurodegenerative Diseases, Berlin
Manuela Thelen
University of Cologne
Stefan J. Teipel
German Center for Neurodegenerative Diseases, Rostock
Ruth Vukovich
German Center for Neurodegenerative Diseases, Gottingen
Michael Wagner
German Center for Neurodegenerative Diseases, Bonn
Emrah Düzel
German Center for Neurodegenerative Diseases, Magdeburg
Frank Jessen
University of Cologne
Henning Boecker
German Center for Neurodegenerative Diseases, Bonn
Lukas Scheef (Lukas.Scheef@dzne.de)
German Center for Neurodegenerative Diseases, Bonn

Research

Keywords: subjective cognitive decline, basal forebrain, CSF biomarker, amyloid, Alzheimer's disease

Posted Date: April 3rd, 2020

DOI: https://doi.org/10.21203/rs.3.rs-20438/v1

Abstract

Background There is growing evidence in the literature that the cholinergic basal forebrain might be one of the earliest affected structures in Alzheimer's disease (AD). Recent data suggest that individuals with preclinical Alzheimer's pathology already show atrophy of the posterior nucleus basalis of Meynert and that this even precedes the atrophy of the entorhinal cortex. Here we investigated whether basal forebrain volume reductions might not only be detectable in the mild cognitive impairment (MCI) and dementia stage of AD, but also in subjective cognitive decline (SCD) individuals who represent an at-risk population for preclinical AD, and examine the relationship with cognitive performance and amyloid-beta pathology. Methods Basal forebrain volumes of 341 participants from the multi-center German Center for Neurodegenerative Diseases Longitudinal Cognitive Impairment and Dementia Study, including 135 healthy controls, 110 SCD, 60 MCI, and 36 AD, were analyzed using high-resolution T1-weighted images. Healthy controls and SCD participants were further grouped into amyloid-positive and amyloid-negative cases according to their cerebrospinal fluid Aβ42/40 ratio. Associations between basal forebrain volume, neuropsychological performance, and amyloid load were evaluated. Results Apart from confirming progressive basal forebrain atrophy from MCI to AD, atrophy of the posterior of nucleus basalis of Meynert was also observed in subjective cognitive decline with confirmed evidence for preclinical Alzheimer's pathology, based on the Aβ42/40 ratio. This atrophy was neither evident in subjects with SCD without amyloid pathology nor in healthy controls with amyloid pathology. Additionally, the volume of the posterior of nucleus basalis of Meynert was significantly correlated with amyloid Aβ42/40 ratio in SCD but not in healthy controls. Conclusion Our results confirm that basal forebrain atrophy occurs early along the Alzheimer's disease trajectory. The observed volume reduction of the cholinergic basal forebrain in Aβ-positive participants with subjective cognitive complains and the absence of any volume reductions in the Aβ-positive healthy controls suggests that these 'subjective cognitive decline' symptoms reflect progression from stage 1 (asymptomatic) to stage 2 (transitional cognitive impairment) of the Alzheimer's continuum (according to the recent National Institute on Aging-Alzheimer's Association Research Framework), revealing the beginning neurodegeneration on a macroscopic level.

1. Introduction

The basal forebrain (BF) provides the major cholinergic projections to cortical and limbic structures [1]. Acetylcholine plays a critical role in learning and memory [2, 3], and cholinergic dysfunction has been suggested to constitute a key factor influencing cognitive decline in Alzheimer's disease (AD) [4, 5]. Post mortem studies in the brains of AD patients have demonstrated severe neurofibrillary degeneration and cell loss within the BF, most prominently in the nucleus basalis of Meynert (NBM) [6, 7]. MRI-based in vivo studies have further revealed severe BF gray matter atrophy in patients with dementia due to AD (DAD) and also in the pre-dementia stage of mild cognitive impairment (MCI) [8, 9]. Cholinergic degeneration has been associated with amyloid deposition in both animal models [10, 11], and human post mortem studies [12, 13]. Using amyloid PET imaging, it was shown that BF atrophy on MRI is linked with cortical amyloid deposition during pre-dementia phases of AD [14]. Recent findings suggest that NBM volume

loss precedes degeneration of the entorhinal cortex, and it is predictive for the longitudinal development of cortical atrophy [15]. Therefore, both basal forebrain neurodegeneration and amyloid pathology seem to be early and critical events in AD progression, which might be interrelated tightly.

While preclinical AD pathology status is often derived from direct amyloid biomarker evidence, there are complementary approaches for identifying at-risk patients, namely clinical examination of individuals with subjective cognitive decline (SCD) [16, 17]. SCD individuals are elderly people who self-report persistent decline in cognitive abilities, despite their objective cognitive performance level still being within normal range. Numerous studies suggest that SCD is associated with an increased likelihood of AD-related biomarker abnormalities and with increased risk of future cognitive decline and developing clinical DAD [18–22]. A recent study found initial evidence that cholinergic BF atrophy is already detectable in cohorts with subjective cognitive complaints [23], and may be associated with both AD biomarkers and a lower cognitive performance trajectory [23, 24]. Especially, SCD in combination with proven AD pathology may reflect progression from stage 1 (asymptomatic) to stage 2 (transitional cognitive impairment) of the Alzheimer's continuum (according to the recent National Institute on Aging-Alzheimer's Association [NIA-AA] Research Framework [25].

A general goal of this study was to investigate cholinergic basal forebrain anatomy across the whole AD spectrum, including SCD (representing an at-risk population for preclinical AD) and healthy controls (HC), within a new, large, multi-center cohort, recruited from memory clinics across Germany, using identical study and MR sequence protocols. CSF biomarker information for a substantial subgroup of this cohort gave us the additional opportunity to explore the interplay between CSF amyloid status and structural changes in SCD and HC which has not been covered in previous studies.

2. Methods

Data were obtained from the German Center for Neurodegenerative Diseases Longitudinal Cognitive Impairment and Dementia Study (DELCODE), an ongoing observational longitudinal memory clinic-based multicenter study focusing on SCD in the context of AD. The DELCODE cohort also includes individuals with MCI and DAD as well as HC subjects without any subjective or objective cognitive impairment. The overall study design is described in detail elsewhere [26].

The DELCODE study protocol was approved by the institutional review boards of all participating sites. All investigations were performed in accordance with the relevant guidelines and regulations. All participants provided written informed consent in accordance with the Declaration of Helsinki.

2.1 Participants

We analyzed cross-sectional data of 135 HC, 110 SCD, 60 MCI and 36 DAD from an interim data release (latest inclusion date: April 2016) who had undergone structural MR imaging, neuropsychological testing, APOE genotyping (ε2/ε3/ε4) and, optionally, lumbar puncture to obtain cerebrospinal fluid (CSF). Lumbar punctures were collected from study participants of all groups who gave informed consent and

showed no medical contraindications for this procedure (Fig. 1). Detailed inclusion and exclusion criteria and group definitions for SCD, MCI and DAD can be found elsewhere [26]. Briefly, SCD was defined if individuals (1) subjectively reported decline of cognitive functioning between the last 6 months and 5 years which (2) caused concern, but (3) participants showed normal performance in the Consortium to Establish a Registry for Alzheimer's disease (CERAD) test battery, as well as Mini Mental State Examination (MMSE) scores ≥ 26. MCI individuals had MMSE score ≥ 24, subjective cognitive decline reported either by the subject, an informant or a clinician, and cognitive performance level being 1.5 standard deviations (SD) below the normal range in the delayed recall trial of the CERAD word list (performance in other CERAD tests could equally fell below the − 1.5 SD threshold, however, a delayed recall deficit was mandatory). With this inclusion criterion, we selected single and multiple-domain amnestic MCI patients, but no non-amnestic MCI patients. Therefore, we use 'MCI' to refer to amnestic MCI patients. DAD patients fulfilled the clinical NINDCS/ADRDA criteria of probable Alzheimer's disease [27].

2.2 Neuropsychological Tests

In order to capture early and subtle cognitive changes in AD development, an extensive neuropsychological test (NPT) battery was applied [26]. To reduce measurement error for single tests and improve sensitivity to early AD-related changes, Confirmatory Factor Analysis (CFA) was used to derive 5 cognitive factors from this NPT battery: learning and memory (MEM), language ability (LANG), executive functions and mental processing speed (EXEC), working memory (WM) and visuo-spatial abilities (VIS) [28]. Further details on the neuropsychological tests can be found in Supplementary Text S1. For each subject, factor scores for each domain were extracted using the regression method [29]. Factor variances and means were fixed to one and zero, respectively. Therefore, the extracted factor score estimates are scaled as z-scores for the performance of the complete sample. Lower scores represent worse performance.

2.3 CSF biomarkers

As CSF biomarker investigations in DELCODE were optional, only about 50% of the participants underwent lumbar puncture. Amyloid β42 (Aβ42) and amyloid β40 (Aβ40) CSF concentrations were determined using commercially available kits according to vendor specifications (V-PLEX Aβ Peptide Panel 1 (6E10) Kit; Mesoscale Diagnostics LLC, Rockville, USA). Because recent studies suggested that CSF Aβ42/40 is a more accurate and sensitive biomarker for MCI and clinical AD compared to Aβ42 alone [30–32], the ratio derived from the literature was used to classify participants as amyloid-positive (Aβ+: Aβ42/Aβ40 ratio < 0.09) or amyloid-negative (Aβ-: Aβ42/Aβ40 ratio ≥ 0.09) [30].

2.4 MRI Acquisition

MRI data were acquired at nine scanning sites, all operating clinical 3T Siemens MR tomographs. High-resolution T1-weighted images were acquired using a magnetization-prepared rapid gradient echo sequence (MPRAGE) which was empirically optimized for optimal gray-white contrast, and standardized

across scanners (TR: 2500 ms, TE: 4.37 ms, flip angle: 7°, IT: 1100 ms, 256 × 256 matrix, FOV: 256 × 256mm^2, slice thickness: 1 mm, 192 sagittal sections without gap covering the whole brain; GRAPPA = 2).

2.5 MRI data processing and BF volume calculation

MRI data were processed and analyzed using the Computational Anatomy Toolbox (CAT12) for SPM12. Preprocessing followed procedures suggested by Kilimann, Grothe [9]. Briefly, MRI scans were automatically segmented into gray matter (GM), white matter and cerebrospinal fluid (CSF) partitions. After segmentation, GM partitions were normalized to the CAT12 default template (IXI555-MNI152), applying modulation for both linear and non-linear normalization. Non-linear normalization was performed using the SPM12 DARTEL algorithm [33].

Measures for the individual BF volumes were obtained by summing up the modulated GM voxel values within a cytoarchitectonic BF atlas in MNI space, which was derived from combined post-mortem MRI and histological data of an autopsy brain [9]. This BF atlas follows Mesulam's nomenclature [1] for dividing the BF into cholinergic nuclei of the medial septal nucleus (Ch1), the vertical nucleus of the diagonal band of Broca (Ch2), its horizontal limb (Ch3), and the nucleus basalis Meynert (NBM, Ch4) with anterior lateral (Ch4al), medial (Ch4am), intermediate (Ch4i) and posterior (Ch4p) subregions. Due to their small sizes, Ch1 and Ch2 were combined into one ROI (Ch1/2), Ch4am and Ch4i into Ch4ai (Fig. 2).

To account for head size differences, the adjusted volumes were calculated from the residuals of a least-square derived linear regression between raw volumes and TIV [34]. TIV was calculated by the summing up the volumes of the GM, white matter, and CSF partitions [35].

2.6 Confirmatory structural analysis

To test for the regional specificity of observed changes in SCD, the volumes of two additional structures, the bilateral caudate nucleus and subgenual cingulate cortex (Brodmann Area [BA] 25), were analyzed, as both are direct vicinity of the BF, but anatomically distinct. The caudate ROIs were taken from the Harvard-Oxford atlas [36], and the BA25 from the DPABI software [37].

To explore potential concurrent alterations in established regions showing early AD-related neurodegeneration, additional analyses focused on hippocampus (total volume, CA1-subfield) [38, 39] and entorhinal cortex [15]. The ROIs were generated using the 'SPM Anatomy Toolbox' [40].

Measures for the individual caudate, BA25, hippocampus (total volume, CA1-subfield) and entorhinal cortex volumes were obtained by summing up the modulated GM voxel values within the ROIs mentioned above. The method of adjusting for TIV was the same as with BF volumes.

2.7 Statistical Analysis

2.7.1 Demographic, clinical and neuropsychological characteristics

Group differences in demographic and clinical data were assessed using Kruskal-Wallis non-parametric tests for continuous measures, and chi-square tests for dichotomous measures. Univariate analyses of covariance (ANCOVA) were used to test significant differences of the neuropsychological tests among the four groups, controlling for age, gender, education in years and APOE status. Pair-wise post hoc t-tests were performed to evaluate cognitive differences between subgroups.

2.7.2 Effects of diagnosis on basal forebrain volumes and relationships with NPT

A univariate Analysis of covariance (ANCOVA) was used to test for significant differences of BF total and subnuclei volumes among the four groups, controlling for potential covariates including age, gender, years of education, APOE4 effects and MRI scanner (dummy-coded). Pair-wise post hoc tests were performed to evaluate volume differences between subgroups.

Partial correlations controlling for the above covariates were used to explore group-wise relationships between BF total and subnuclei volumes, respectively, and the 5 cognitive factor scores.

2.7.3 Effects of amyloid status in SCD and HC on BF volume

Main and interaction effects of the factors amyloid status (Aβ+/Aβ-) and diagnostic group (HC/SCD) on the BF volumes were assessed using an ANCOVA, controlling for age, gender, years of education, APOE4 effects, and scanners. Follow-up pairwise comparisons included: SCD^+ vs SCD^-, HC^+ vs HC^-, HC^+ vs SCD^+ and HC^- vs SCD^-. Finally, the within-subgroup relationships between the regional BF volumes, continuous Aß42/40 ratio, and the 5 cognitive factors, respectively, were explored using partial correlations (covariates as above).

2.7.4 Confirmatory structural analysis: Effects of amyloid status in SCD and HC on additional regions

Main and interaction effects of the factors amyloid status (Aβ+/Aβ-) and diagnostic group (HC/SCD) on the caudate/BA25, hippocampus (total volume, CA1-subfield) and entorhinal cortex volumes were assessed using an ANCOVA controlling for age, gender, years of education, APOE4 effects, and scanner. Follow-up pairwise comparisons included: SCD^+ vs SCD^-, HC^+ vs HC^-, HC^+ vs SCD^+ and HC^- vs SCD^-.

2.7.5 Exploratory analysis: Effects of amyloid status in MCI and HC on BF volume

In order to explore the role of amyloid status in the clinical samples, we also assessed the main and interaction effects of the factors amyloid status (Aβ+/Aβ-) and diagnostic group (HC/MCI) on the BF volumes by using an ANCOVA (covariates as above). Follow-up pairwise comparisons included: MCI^+ vs MCI^-, HC^+ vs HC^-,HC^+ vs MCI^+ and HC^- vs MCI^-. The sample size for the DAD patients (N = 17, Fig. 1, N_{AD+}=16 and N_{AD-}=1) was too small for reliable analyses.

All statistical tests were two-tailed, and the statistical significance level was set at $p < 0.05$ (Bonferroni-corrected), except for exploratory partial correlation analyses where an uncorrected threshold of $p < 0.05$ was chosen. Missing data were treated using pairwise deletion. All statistical analyses were performed using SPSS Statistics v22.0 (IBM, Armonk, NY, USA).

3. Results

3.1 Demographic, clinical and neuropsychological test characteristics

The demographic characteristics as well as the NPT results are summarized in Table 1. The four groups differed significantly in age, gender, education, APOE4 genotype, clinical measures (MMSE, Clinical Dementia Rating Score (CDR)-global, CDR-sum of box (CDR-SOB)), as well as the five cognitive factors. Age in DAD and MCI was significantly higher than in HC. APOE-ε4 carriers were significantly less frequent in HC than in MCI and DAD. Years of education were significantly lower in DAD than in HC, and the proportion of male participants was significantly higher in MCI than in HC. Compared to SCD, HC were slightly younger, and included significantly fewer APOE-ε4 carriers. In line with the inclusion criteria, MCI and DAD showed significant lower scores on the MMSE and on all five cognitive factors. The MMSE showed no significant differences between HC and SCD, but the CDR Sum of Boxes (CDR-SOB) and the CDR-global score in SCD was significantly higher than in HC (Table 1).

Table 1: Demographic, clinical and neuropsychological characteristic for HC, SCD, MCI and DAD groups

	HC (n = 135)	SCD (n= 110)	MCI (n=60)	DAD (n=36)	P value	Post-hoc comparisons
Age(yrs)	68.7 ± 5.2	71.3 ± 5.7	73.1 ± 5.0	73.3 ± 7.0	<0.001[a]	HC < AD*** HC < MCI*** HC < SCD**
Gender (M/F)	55/80 (0.41)	53/57(0.48)	38/22(0.63)	16/20(0.44)	=0.03[b]	HC < MCI*
Education(yrs.)	14.9 ± 2.8	14.6 ± 3.2	$14.1 \pm 3.2_1$	13.1 ± 3.2	=0.009 [a]	AD < HC*
MMSE	$29.4 \pm 0.9_1$	29.2 ± 1.0	28.1 ± 1.6	23.6 ± 3.4	<0.001[a]	AD < MCI*** AD < SCD*** AD < HC*** MCI< SCD*** MCI< HC***
CDR-SOB	0.0 ± 0.1	0.3 ± 0.4	1.5 ± 1.2	4.8 ± 1.4	<0.001[a]	AD > MCI* AD > SCD*** AD > HC*** MCI > HC*** MCI > SCD*** SCD > HC***
CDR-global	0.0 ± 0.0	0.2 ± 0.3	0.5 ± 0.1	0.9 ± 0.2	<0.001[a]	AD > SCD*** AD > HC*** MCI > HC*** MCI > SCD*** SCD > HC***
MEM factor score	0.6 ± 0.1 (-0.8/1.3)	$0.4 \pm 0.1_1$ (-1.3/1.3)	-0.6 ± 0.1 (-1.9/0.7)	-2.1 ± 0.1 (-3.0/-1.4)	<0.001[c]	AD < MCI*** AD < SCD*** AD < HC*** MCI< SCD*** MCI< HC***
LANG factor score	0.5 ± 0.5 (-0.6/1.9)	$0.3 \pm 0.6_1$ (-1.6/1.6)	-0.6 ± 0.7 (-2.2/0.8)	-1.9 ± 0.7 (-3.6/-0.8)	<0.001[c]	AD < MCI*** AD < SCD*** AD < HC*** MCI< SCD*** MCI< HC***
EXEC factor score	0.5 ± 0.5 (-0.9/1.8)	$0.3 \pm 0.7_1$ (-1.6/1.7)	-0.5 ± 0.8 (-2.6/0.8)	-1.9 ± 0.9 (-3.8/-0.3)	<0.001[c]	AD < MCI*** AD < SCD*** AD < HC*** MCI < SCD*** MCI < HC***
WM factor score	0.3 ± 0.6 (-0.9/1.9)	$0.3 \pm 0.7_1$ (-1.4/-1.7)	-0.4 ± 0.8 (-2.0/1.1)	-1.5 ± 0.9 (-3.5/0.3)	<0.001[c]	AD < MCI*** AD < SCD*** AD < HC*** MCI < SCD*** MCI < HC***
VIS factor score	0.3 ± 0.4 (-1.3/1.1)	$0.2 \pm 0.5_1$ (-1.4/1.1)	-0.3 ± 0.8 (-3.0/0.7)	-1.5 ± 1.5 (-6.7/0.2)	<0.001[c]	AD < MCI*** AD < SCD*** AD < HC*** MCI < SCD*** MCI < HC***
APOE(*ε4/non-4*)	$23/109_3$(17.4)	$36/72_2$ (33.3)	21/39(35.0)	$25/10_1$ (71.4)	<0.001 [b]	HC < SCD* HC < AD*** HC < MCI* HC< SCD* SCD < AD*** MCI < AD**

Values are represented with mean ± standard deviation and number with percentage. Subscripts denote number of missing values. The numbers in the brackets of cognitive five factors are the minimum and maximum for the score. HC, Healthy Control; SCD, Subjective Cognitive Decline; MCI, Mild Cognitive Decline; DAD, Dementia due to Alzheimer's type; MMSE, Mini-Mental State Examination; CDR: Clinical Dementia Ratings; CDR-SOB:

CDR sum of boxes score; MEM, Learning and memory; LANG, Language; EXEC, Executive and speed function; WM, working memory; VIS, Visuospatial Function; [a] Kruskal-Wallis Non-Parameter Test; [b] Chi-Square Test. [c] ANCOVA Test controlling for age, gender, years in education and APOE4 status. Post hoc Bonferroni-corrected p-value: * p-value < 0.05, ** Bonferroni-corrected p-value < 0.01, *** p-value <0.001;

3.2 Effects of diagnosis on basal forebrain volumes and relationships with NPT

The volumes of the BF and its subnuclei differed significantly across the four groups (Table 2). BF volume in the DAD subjects was significantly lower in all subnuclei compared to subjects with MCI and SCD as well as HC. Comparing MCI with SCD and HC, the total BF and Ch4p as well as Ch4al regions showed a significant volume reduction in the MCI group. When comparing SCD and HC, we found no significant differences for total BF volume and any of the subnuclei.

Partial correlation analyses revealed significant associations between total BF volume and MEM (r = 0.433, p = 0.002) as well as LANG (r = 0.383, p = 0.007) in the MCI group, but not in the DAD group. The same held true for the subnuclei. We found significant associations for Ch4p and Ch4al volumes with MEM (Ch4p, r = 0.443, p = 0.001; Ch4al, r = 0.354, p = 0.013) as well as LANG (Ch4p, r = 0.428, p = 0.002; Ch4al, r = 0.345, p = 0.015) for the MCI group only. For SCD we solely found a correlation between Ch4ai and visuo-spatial cognition, and this was only observed at trend level (r = 0.19; p = 0.063).

Table 2: Basal forebrain volumes and its subregions across HC, SCD, MCI and DAD

	HC [mm^3]	SCD [mm^3]	MCI [mm^3]	AD [mm^3]	P-value	Post-hoc comparisons
BF	596.5 ± 4.9	596.0 ± 5.2	568.8 ± 7.0	504.5 ± 9.4	<0.001	AD < MCI*** AD < SCD*** AD < HC*** MCI< HC* MCI< SCD*
Ch1/2	82.5 ± 0.8	84.4 ± 0.9	80.3 ± 1.1	75.3 ± 1.5	<0.001	AD < SCD*** AD < HC*** AD < MCI*
Ch3	146.0 ± 1.4	150.3 ± 1.5	147.0 ± 2.0	131.1 ± 2.7	<0.001	AD < MCI*** AD < SCD*** AD < HC***
Ch4ai	143.3 ± 1.5	141.6 ± 1.6	138.5 ± 2.2	119.4 ± 2.9	<0.001	AD < MCI*** AD < SCD*** AD < HC***
Ch4al	113.8 ± 1.1	114.6 ± 1.1	107.5 ± 1.5	101.0 ± 2.0	<0.001	AD < SCD*** AD < HC*** AD < MCI* MCI< HC** MCI< SCD**
Ch4p	100.1 ± 1.2	98.6 ± 1.2	89.3 ± 1.6	72.2 ± 2.2	<0.001	AD < MCI*** AD < SCD*** AD < HC*** MCI< HC*** MCI< SCD***

Basal forebrain atrophy patter across the four groups using ANCOVA analysis controlled all covariates including age, gender, years in education, MRI scanner and APOE4 status. Values are represented with estimated marginal means ± standard error. HC: healthy control; SCD: Subjective Cognitive Decline; MCI: Mild Cognitive Decline; DAD: Dementia due to Alzheimer's type. Post-hoc comparisons (*Bonferroni-corrected p-value < 0.05, ** Bonferroni-corrected p-value < 0.01, *** Bonferroni-corrected p-value < 0.001).

3.3 Effects of amyloid status in SCD and HC on BF volume

All HC and SCD participants with both structural scans and CSF biomarker available were selected, with 38% (16 of 42) SCD and 27% (13 of 48) HC being categorized Aβ+ (Aβ42/40 < 0.09). The background characteristics of the participants with or without available CSF amyloid status did not differ significantly, neither in SCD nor in the HC group (Table S1). Demographic and neuropsychological characteristic for amyloid-stratified HC and SCD subgroups were also shown in supplementary Table S2. ANCOVA revealed a main effect of CSF amyloid status (Aβ+/Aβ-: $F_{1,74} = 4.676$, p = 0.034) on Ch4p volume which was qualified by a significant interaction between CSF amyloid status and SCD status ($F_{1,74} = 4.186$, p = 0.044; Fig. 3). The Ch4p volume was significantly smaller in amyloid-positive compared to amyloid-negative SCD participants ($Ch4p_{SCD}^{+} = 92.18 \pm 3.04\ mm^3$, $Ch4p_{SCD}^{-} = 103.17 \pm 2.21\ mm^3$; $F_{1,74} = 7.964$, p = 0.006, Partial $\eta^2 = 0.097$). Critically, the Ch4p volume in the SCD + group was even significantly smaller than in the amyloid-positive control group ($Ch4p,_{HC}^{+} = 101.48 \pm 2.95 mm^3$, $F_{1,74} = 4.791$, p = 0.032, Partial

$\eta^2 = 0.06$), while the latter did not differ significantly from amyloid-negative controls (Ch4p, $_{HC}^{-}$ = 102.25 ± 1.86 mm^3; $F_{1,74} = 0.049$, $p = 0.83$, Partial $\eta^2 = 0.001$). No significant main or interaction effects of amyloid status were found for either total BF volume or the volumes of the other subnuclei (Table S3).

Complementary to the categorical analysis of Ch4p volume differences, partial correlation analyses revealed a correlation between the Aβ42/40 ratio and the Ch4p volume in the SCD subsample with CSF measures, whereas the correlation was not significant in the control group ($r_{SCD} = 0.365$, $p = 0.044$; $r_{HC} = -0.041$, $p = 0.805$; Fig. 4). Partial correlation analysis revealed no significant correlation between Ch4p and any of the 5 cognitive factors in SCD subsample (all $p > 0.371$).

3.4 Confirmatory structural analysis: Effects of amyloid status in SCD and HC on additional regions

None of the explorative ROI analyses (caudate nucleus, BA25, hippocampus total volume, CA1-subfield volume, entorhinal cortex) revealed significant main effects of SCD status or amyloid status. Furthermore, no significant interaction effects between CSF amyloid status and SCD status were found (Table S4).

3.5 Exploratory analysis: Effects of amyloid status in MCI and HC on BF volume

MCI participants with both structural scans and CSF biomarker available were selected, with 60% (18 of 30) MCI being categorized Aβ+ (Aβ42/40 < 0.09). We only found a significant main effect of MCI status on Ch4p and Ch4al subregions (Ch4p: $F_{1,64} = 10.61$, $p = 0.002$; Ch4al: $F_{1,64} = 4.15$, $p = 0.046$) (Table S5). The Ch4p and Ch4al volume were significantly smaller in MCI subsample compared to HC subsample (Table S5). Moreover, there was no main effect of amyloid on total BF volume or on the volumes of the other subnuclei (Table S5). No significant interaction effects of amyloid status and MCI status were found for either total BF volume or the volumes of the other subnuclei (Table S5).

Discussion

We present the first study that directly compared BF volumes of HC, SCD, MCI and DAD patients in a large multi-center dataset. We found a significant effect of diagnosis on BF total and subnuclei volumes, which was most pronounced in Ch4p. In patients with clinically manifest DAD, almost all BF subnuclei were affected by volume reduction, whereas in MCI patients, volume reduction was yet confined to Ch4al and Ch4p. Moreover, Ch4p volume correlated significantly with cognitive performance measures (MEM and LANG) in participants with MCI. In the subgroup with available CSF amyloid markers, an interaction between diagnosis (SCD vs. HC) and CSF amyloid status was observed in the cognitively normal subgroups, indicating Ch4p volume reductions only in amyloid-positive SCD (but not amyloid-positive HC), which also showed linear positive correlations with Aβ42/40 ratios in the SCD subgroup, but not in the controls.

Our findings are consistent with the assumption that incipient BF atrophy already begins in individuals with preclinical AD pathology. BF atrophy most likely starts in Ch4p and subsequently spreads across the entire brain with progressing disease. Notably, the fact amyloid-positive HC subjects did not show comparable levels of BF atrophy, suggests that they present an earlier AD disease stage (NIA-AA stage 1) than the amyloid-positive individuals with SCD, whose cognitive complaints may already reflect subtle cognitive deterioration (NIA-AA stage 2), which may in turn be related to an early cholinergic deficit.

In accordance with previous *in vivo* MRI morphometric studies [9, 41], we found significant volume reductions of the BF and in most of its subregions in DAD patients. This is in line with previous *post mortem* studies in DAD, which have demonstrated that severe neurofibrillary degeneration and neuronal loss in the cholinergic BF, leading to reduced cholinergic innervation of the cerebral cortex [6, 7]. In addition, BF volume loss was most pronounced in the Ch4p subregion. This converges with histopathological data from DAD patients showing that, while the entire BF is affected by cell loss, neurodegeneration is most severe in Ch4p [42]. This observation mirrors the functional neuroanatomy of cholinergic modulation of cortical activity in AD, which is particularly affected in the superior temporal gyrus and temporal pole, key targets of the cholinergic projections from Ch4p [1, 43]. Unlike other BF subnuclei, Ch4p and Ch4al exhibited volume loss already in MCI patients, confirming earlier *in vivo* MRI studies [8], and providing evidence that the cholinergic BF subregions are not uniformly affected during earlier stages of AD progression. Instead, the posterior part of the NBM, Ch4p, appears to be most vulnerable to AD pathology. While this interpretation remains tentative owing to the cross-sectional nature of our data, this would be consistent with a recent study [15] which found longitudinal NBM, but not entorhinal atrophy progression over a two-year period already in healthy individuals with preclinical amyloid pathology, suggesting very early BF involvement in AD pathogenesis.

Our findings are compatible with the latter view by showing that Ch4p volume reductions are present in amyloid-positive SCD, while no atrophic changes were detectable in the entorhinal (and also hippocampal) areas. Neither SCD on its own, nor CSF amyloid pathology in clinically normal individuals were associated with NBM atrophy, while their combination was. While the lack of BF atrophy in healthy controls with amyloid pathology appears to contradict the abovementioned study [15], it has to be noted that their observations were based on longitudinal data over two years which may be more sensitive to detect degenerative processes in this early disease stage. Our notion that the simultaneous presence of amyloid pathology *plus* SCD symptoms reflects an advanced stage of preclinical AD is compatible with Vogel, Varga Dolezalova [44] who observed that cortical Aβ accumulation as assessed with PiB positron emission tomography (PET) and clinical SCD predicted cognitive decline in a complementary manner [45]. This is also in line with an increased hippocampal atrophy and lower cognitive performance in SCD with positive APOE status [46], even though APOE constitutes a risk factor rather than a biomarker for amyloid pathology. Taken together with findings that Ch4p volume loss precedes entorhinal atrophy and mediates longitudinal memory loss [15], one might conclude from our findings that SCD in amyloid-positive individuals constitutes a very early clinical manifestation of an AD-related cholinergic neuronal loss that cannot be fully compensated anymore, thereby leading to first symptoms of incipient cognitive decline.

This view is also supported by our correlation analyses showing that Ch4p volume decreases with increasing amyloid pathology as indexed by CSF Aβ ratios in SCD subsample. The relationship between amyloid pathology and BF atrophy is also supported by the literature. Cortical amyloid accumulation correlates with cholinergic system atrophy, as shown in animal models [3, 10] and *post mortem* studies in humans [12, 13]. The strong association between Ch4p atrophy and Aβ42/40 ratio in individuals with SCD may reflect downstream neurotoxic effects of amyloid aggregates and vulnerability of Ch4p cholinergic cells to amyloid-related neurodegeneration, which may trigger incipient functional impairments in innervated brain regions. This is compatible with previous findings showing that Ch4p volume reductions in SCD correlated with reduced glucose metabolism in the precuneus [23]. Reduced precuneus glucose metabolism has previously been suggested to constitute a highly sensitive biomarker for AD [47, 48], and in MCI, it is associated with a conversion rate toward DAD of more than 90% within two years [49, 50]. The AD-related early atrophy of Ch4p might also explain why individuals with both SCD and biomarker evidence for AD are at increased risk of future cognitive decline and progression to MCI and ultimately DAD [51-55], as in these individuals, Ch4p degradation has already started.

Interestingly, exploratory analyses for MCI patients did not reveal a significant interaction with CSF amyloid status, neither for the volume of Ch4p, nor other BF subnuclei. Even though surprising on a first view, this missing association was also reported by other groups [56]. They might suggest that at the earlier SCD stadium the amyloid deposition is the driving force, whereas at a later stage, the atrophy is more likely driven by other factors than amyloid. However, a more detailed analysis including tau and other biomarkers would be needed to further prove this hypothesis. Moreover, the reduced sample size and the cross-sectional nature of the imaging data may have precluded the detection of more subtle effects: Actually, a recent longitudinal study contrasting a large sample of amyloid-positive MCI individuals with amyloid-negative healthy controls found not only higher volume losses in the NBM (Ch4), but also in the medial septal nucleus/diagonal band of Broca of the MCI patients [57].

The lack of associations between BF volumes and cognitive domain scores in the clinically unimpaired HC and SCD groups is consistent with an earlier study in healthy elderly that found no correlations with specific neuropsychological measures, except for a positive association with a global intelligence score [58, 59] . Meanwhile, the linear relationships between volume loss of Ch4p and decline in memory and language performance within the MCI sample is partially consistent with a previous study that observed significant correlations of total BF volume with memory and executive test scores, respectively [59]. This suggests that the loss of cholinergic innervation due to NBM neurodegeneration may contribute to the decline of cognitive functioning during this disease stage, although we must note the exploratory nature of these finding due to the uncorrected significance threshold. The lack of complementary correlations in DAD patients seems inconsistent with a recent study with DAD patients under cholinesterase inhibitor treatment which observed significant associations between total BF volume and global cognition, as well as memory and executive functions [60]. Meanwhile, the current sample was much smaller, limiting the statistical power of the present analyses.

One potential methodological limitation of the present study is related to the limited spatial resolution of our MRI-based basal forebrain volumetry, considering the small size of the BF nuclei compared with the spatial resolution, image contrast, and the atlas used, which is based on *post mortem* data from one single subject. It should be noted, though, that the locations of the BF nuclei derived from this atlas are in good agreement with a cytoarchitectonical probability map derived from ten subjects [8, 9, 61]. Furthermore, even though the MR method is relatively coarse, spatial specificity is still high enough to assess basal forebrain anatomy sufficiently. Another limitation is that volumetric approaches can, unlike histopathological methods, not distinguish between cell shrinkage, cell death, glial or neural loss or reduction of extracellular space, Therefore, interpretations in terms of 'atrophy' or 'volume loss' remain debatable. Nevertheless, considering previous histopathological findings in the context of our MRI-based findings, neurodegeneration in the BF is the most likely interpretation of our results. The fact that volume changes were observed in the BF regions of interest, but not in proximal control regions (caudate, BA25), also argues against global effects, and for spatial specificity of our findings. Moreover, the limited CSF sample size precluded further subdivision according to both amyloid and tau pathology in this interim analysis. We note that exploratory analyses according to tau pathology **(Supplement Table S6/Table S7)** showed no significant effects. Dual stratification will probably become possible with future extensions of the dataset. Finally, as longitudinal MRI and cognitive data were not yet available for analysis, our cross-sectional approach could not track BF volume changes over time, which limits sensitivity to detect atrophic processes.

Despite these methodological caveats, important strengths of this study are the longitudinal multicentric study design, the relatively large group size, the availability of biomarkers and a broad neuropsychological test battery that was specifically designed to characterize SCD as broadly as possible. While longitudinal follow-up data collection is still evolving, it will be important to investigate the longitudinal trajectory of BF changes, its relation to evolving alterations of other brain structures like the entorhinal cortex and hippocampus as well as to cognitive decline, and to assess its predictive value for the conversion of SCD into MCI and ultimately DAD.

Conclusions

To conclude, our results support progression of basal forebrain atrophy along the AD trajectory, with Ch4p atrophy emerging already at an early stage of AD pathogenesis. The subjective cognitive complaints in amyloid-positive SCD may reflect joint detrimental effects of amyloid pathology and incipient Ch4p alterations, right at the border when these underlying pathologies cannot be fully compensated, hence leading to initial (subjective) symptoms. Therefore, they seem to be a more promising target population for AD prevention/intervention trials than 'pure' amyloid-positive populations or SCD populations as such. Researchers are clearly reminded that the clinical SCD concept is, at least for the time being, primarily an enrichment strategy, not a preclinical AD stage on its own. AD-related biomarkers are needed to further disentangle this population.

Abbreviations

AD	Alzheimer's Disease
MCI	Mild Cognitive Decline
SCD	Subjective Cognitive Decline
HC	Healthy Controls
DAD	Dementia due to Alzheimer's Disease
DELCODE	DZNE – Longitudinal Cognitive Impairment and Dementia Study
Aβ42/40	Amyloid-beta 40/ Amyloid-beta 42
BF	Basal forebrain
MRI	Magnetic Resonance Imaging
NIA-AA	National Institute on Aging-Alzheimer's Association
CSF	Cerebrospinal fluid
APOE	Apolipoprotein
CDR	Clinical Dementia Rating
SOB	Sum of box
CERAD	Consortium to Establish a Registry for Alzheimer's disease
MMSE	Mini Mental State Examination
SD	Standard deviations
NINDCS	National Institute of Neurological and Communicative Disorders and Stroke
ADRDA	Alzheimer's Disease and Related Disorders Association
NPT	Neuropsychological test
CFA	Confirmatory Factor Analysis
MEM	Learning and Memory
LANG	Language

EXEC	Executive functions and mental processing speed
WM	Working Memory
VIS	Visuo-spatial abilities
MPRAGE	Magnetization-prepared rapid gradient echo sequence
TE	Echo time
TI	Inversion Time
TR	Repetition time
FOV	Field of View
GM	Gray Matter
DARTEL	Diffeomorphic Anatomical Registration Through Exponentiated Lie Algebra
GRAPPA	Generalized Autocalibrating Partial Parallel Acquisition
MNI	Montreal Neurological Institute
IXI	Information eXtraction from Images
Ch1	Medial septal nucleus
Ch2	Vertical nucleus of the diagonal band of Broca
Ch3	Horizontal limb of the diagonal band of Broca
NBM/Ch4	Nucleus Basalis Meynert
Ch4al	Anterior lateral of Nucleus Basalis Meynert
Ch4am	Medial of Nucleus Basalis Meynert
Ch4i	Intermediate of Nucleus Basalis Meynert
Ch4p	Posterior of Nucleus Basalis Meynert
TIV	Total Intracranial Volume
BA	Brodmann Area
DPABI	Data Processing & Analysis for Brain Imaging

ROI	Region of Interest
ANCOVA	Univariate analyses of covariance
PiB	Pittsburgh compound B
PET	Positron emission tomography

Declarations

Ethics approval and consent to participation:

DELCODE were approved by the institutional review boards of all participating sites (Charité Berlin, Bonn, Cologne, Ludwig-Maximilians-University Munich, Rostock, and Tübingen), and coordinated by the ethics committee of the medical faculty of the University of Bonn, under the registration number: 117/13. All procedures were performed in accordance with the relevant guidelines and regulations. All participants provided written informed consent.

Consent for publication:

Not applicable.

Availability of data and materials:

The data which support this study are not publicly available, but may be provided upon reasonable request.

Competing interests:

The authors declare that they have no competing interest.

Funding:

The study was funded by the German Center for Neurodegenerative Diseases (Deutsches Zentrum für Neurodegenerative Erkrankungen, DZNE), Reference number BN012.

Authors' contributions:

Overall design and implementation: FJ, A. Spottke, HB, KB, ED, KF, MTH, CL, OP, JP, AR, A. Schneider, SJT, MT, MW. Conducting the study at the respective sites: KB, CC, CF, EII, KF, IK, CL, CDM, MM, OP, LP, JP, A. Schneider, BHS, EJS, SJT, RV. Methodological core data management and analyses: FB, ED, LD, MTH, LK, AR, MW, SW. Data analysis: SL; Supervision of data analyses: LS, MJG. Data interpretation: SL, LS, MD. Writing of the manuscript draft: SL. Critical revisions of the manuscript draft: LS, MD. All authors critically reviewed and approved the final manuscript.

Acknowledgements:

We would like to thank all the researchers in the DELCODE study and acknowledge the altruism of the DELCODE participants and their families.

Delcode Study Group

J. Acosta-Cabonero, S. Altenstein, H. Amthauer, I. Apostolova, M. Barkhoff, C. Bartels, D. Berron, M. Betts, M. Beuth, D. Bittner, H. Boecker, F. Brosseron, K. Brüggen, M. Buchmann, K. Bürger, A. Cardenas-Blanco, C. Catak, Y. Cheng, L. Coloma Andrews, M. Daamen, M. Dichgans, L. Dobisch, A. Dörr, E. Düzel, M. Dyrba, M. Ehrlich, B. Ertl-Wagner, J. Faber, K. Fließbach, D. Frimmer, I. Frommann, M. Fuentes , D. Grieger-Klose, D. Hartmann, D. Hauser, T. Heger, C. Heine, J. Henf, G. Hennes, G. Herrmann, P. Hinderer, S. Hirschel, B. Huber, A. Hufen, H. Janecek-Meyer, D. Janowitz, F. Jessen, C. Kainz, P. Kalbhen, E. Kasper, I. Kilimann, C. Kindler, X. Kobeleva, B. Kofler, C. Korp, M. Kreißl, M. Kreuzer , E. Kuder-Buletta, A. Langenfurth , C. Laske, E. Lau, C. Lindlar, K. Lindner, A. Lohse, E. Markov, H. Megges, F. Menne, C. D. Metzger, E. Meyer, L. Miebach, K. Möhring, A. Müller, C. Müller, C. Mychajliw, P. Nestor, K. Neumann, S. Nuhn, O. Peters, H. Pfaff, I. Pfahlert, A. Polcher, J. Priller, K. Radenbach, H. Raum, L. Rausch, A. Rominger, S. Röske, C. Ruß, P. Sabik, A. Sagebiel, Y. Sagik, P. Sänger, J. Schmid, M. Schmidt, A. Schneider, H. Schulz, F. Schulze, P. Schulze , H. Schütze, S. Schwarzenboeck, A. Seegerer, O. Speck, A. Spottke, E. J. Spruth, J. Stephan, A. Szagarus, S. J. Teipel, C. Tempelmann, I. Villar Munoz , I. Vogt, M. Wagner, M.-A. Weber, G. Wenzel, C. Werner, S. Weschke, C. Westerteicher, C. Widmann, I. Wienhöft, J. Wiltfang, J. Wizenhausen, S. Wolfsgruber, R. Yakupov, L. Zabel, H. Zech, G. Ziegler, A. Zollver.

References

1. Mesulam, M.M., et al., *Cholinergic innervation of cortex by the basal forebrain: cytochemistry and cortical connections of the septal area, diagonal band nuclei, nucleus basalis (substantia innominata), and hypothalamus in the rhesus monkey.* J Comp Neurol, 1983. **214**(2): p. 170-97.
2. Baxter, M.G., et al., *Selective immunotoxic lesions of basal forebrain cholinergic cells: effects on learning and memory in rats.* Behav Neurosci, 2013. **127**(5): p. 619-27.
3. Bohnen, N.I., et al., *Recent advances in cholinergic imaging and cognitive decline-Revisiting the cholinergic hypothesis of dementia.* Curr Geriatr Rep, 2018. **7**(1): p. 1-11.
4. Baskin, D.S., et al., *Brain choline acetyltransferase and mental function in Alzheimer disease.* Arch Neurol, 1999. **56**(9): p. 1121-3.
5. Pappas, B.A., et al., *Choline acetyltransferase activity and cognitive domain scores of Alzheimer's patients.* Neurobiol Aging, 2000. **21**(1): p. 11-7.
6. Whitehouse, P.J., et al., *Alzheimer's disease and senile dementia: loss of neurons in the basal forebrain.* Science, 1982. **215**(4537): p. 1237-9.
7. Vogels, O.J., et al., *Cell loss and shrinkage in the nucleus basalis Meynert complex in Alzheimer's disease.* Neurobiol Aging, 1990. **11**(1): p. 3-13.

8. Grothe, M., et al., *Reduction of basal forebrain cholinergic system parallels cognitive impairment in patients at high risk of developing Alzheimer's disease.* Cereb Cortex, 2010. **20**(7): p. 1685-95.
9. Kilimann, I., et al., *Subregional basal forebrain atrophy in Alzheimer's disease: a multicenter study.* J Alzheimers Dis, 2014. **40**(3): p. 687-700.
10. Beach, T.G., *Physiologic origins of age-related beta-amyloid deposition.* Neurodegener Dis, 2008. **5**(3-4): p. 143-5.
11. Boncristiano, S., et al., *Cholinergic changes in the APP23 transgenic mouse model of cerebral amyloidosis.* J Neurosci, 2002. **22**(8): p. 3234-43.
12. Arendt, T., et al., *Neuronal loss in different parts of the nucleus basalis is related to neuritic plaque formation in cortical target areas in Alzheimer's disease.* Neuroscience, 1985. **14**(1): p. 1-14.
13. Potter, P.E., et al., *Pre- and post-synaptic cortical cholinergic deficits are proportional to amyloid plaque presence and density at preclinical stages of Alzheimer's disease.* Acta Neuropathol, 2011. **122**(1): p. 49-60.
14. Grothe, M.J., et al., *Basal forebrain atrophy and cortical amyloid deposition in nondemented elderly subjects.* Alzheimers Dement, 2014. **10**(5 Suppl): p. S344-53.
15. Schmitz, T.W., R. Nathan Spreng, and I. Alzheimer's Disease Neuroimaging, *Basal forebrain degeneration precedes and predicts the cortical spread of Alzheimer's pathology.* Nat Commun, 2016. **7**: p. 13249.
16. Jessen, F., et al., *A conceptual framework for research on subjective cognitive decline in preclinical Alzheimer's disease.* Alzheimers Dement, 2014. **10**(6): p. 844-52.
17. Studart, A.N. and R. Nitrini, *Subjective cognitive decline: The first clinical manifestation of Alzheimer's disease?* Dement Neuropsychol, 2016. **10**(3): p. 170-177.
18. Dufouil, C., et al., *APOE genotype, cholesterol level, lipid-lowering treatment, and dementia: the Three-City Study.* Neurology, 2005. **64**(9): p. 1531-8.
19. van Oijen, M., et al., *Subjective memory complaints, education, and risk of Alzheimer's disease.* Alzheimers Dement, 2007. **3**(2): p. 92-7.
20. Jessen, F., et al., *Prediction of dementia by subjective memory impairment: effects of severity and temporal association with cognitive impairment.* Arch Gen Psychiatry, 2010. **67**(4): p. 414-22.
21. Reisberg, B., et al., *Outcome over seven years of healthy adults with and without subjective cognitive impairment.* Alzheimers Dement, 2010. **6**(1): p. 11-24.
22. Scheef, L., et al., *Glucose metabolism, gray matter structure, and memory decline in subjective memory impairment.* Neurology, 2012. **79**(13): p. 1332-9.
23. Scheef, L., et al., *Subregional volume reduction of the cholinergic forebrain in subjective cognitive decline (SCD).* Neuroimage Clin, 2019. **21**: p. 101612.
24. Teipel, S.J., et al., *Effect of Alzheimer's disease risk and protective factors on cognitive trajectories in subjective memory complainers: An INSIGHT-preAD study.* Alzheimers Dement, 2018. **14**(9): p. 1126-1136.

25. Jack, C.R., Jr., et al., *NIA-AA Research Framework: Toward a biological definition of Alzheimer's disease.* Alzheimers Dement, 2018. **14**(4): p. 535-562.
26. Jessen, F., et al., *Design and first baseline data of the DZNE multicenter observational study on predementia Alzheimer's disease (DELCODE).* Alzheimers Res Ther, 2018. **10**(1): p. 15.
27. McKhann, G.M., et al., *The diagnosis of dementia due to Alzheimer's disease: recommendations from the National Institute on Aging-Alzheimer's Association workgroups on diagnostic guidelines for Alzheimer's disease.* Alzheimers Dement, 2011. **7**(3): p. 263-9.
28. Wolfsgruber, S., L. Kleineidam, J. Guski, O. Peters, K. Buerger, M. Ewers, J. Priller, C. Laske, S. J. Teipel, K. Fließbach, A. Schneider, A. Spottke, F. Jessen and M. Wagner *Latent-factor structure of the DELCODE study neuropsychological test battery* Alzheimer's & Dementia: The Journal of the Alzheimer's Association 2017. **13**(7): p. P1136-P1137.
29. Grice, J.W., *Computing and evaluating factor scores.* Psychol Methods, 2001. **6**(4): p. 430-50.
30. Janelidze, S., et al., *CSF Abeta42/Abeta40 and Abeta42/Abeta38 ratios: better diagnostic markers of Alzheimer disease.* Ann Clin Transl Neurol, 2016. **3**(3): p. 154-65.
31. Hansson, O., et al., *Prediction of Alzheimer's disease using the CSF Abeta42/Abeta40 ratio in patients with mild cognitive impairment.* Dement Geriatr Cogn Disord, 2007. **23**(5): p. 316-20.
32. Lewczuk, P., et al., *Cerebrospinal Fluid Abeta42/40 Corresponds Better than Abeta42 to Amyloid PET in Alzheimer's Disease.* J Alzheimers Dis, 2017. **55**(2): p. 813-822.
33. Ashburner, J., *A fast diffeomorphic image registration algorithm.* Neuroimage, 2007. **38**(1): p. 95-113.
34. Voevodskaya, O., et al., *The effects of intracranial volume adjustment approaches on multiple regional MRI volumes in healthy aging and Alzheimer's disease.* Front Aging Neurosci, 2014. **6**: p. 264.
35. Malone, I.B., et al., *Accurate automatic estimation of total intracranial volume: a nuisance variable with less nuisance.* Neuroimage, 2015. **104**: p. 366-72.
36. Makris, N., et al., *Decreased volume of left and total anterior insular lobule in schizophrenia.* Schizophr Res, 2006. **83**(2-3): p. 155-71.
37. Yan, C.G., et al., *DPABI: Data Processing & Analysis for (Resting-State) Brain Imaging.* Neuroinformatics, 2016. **14**(3): p. 339-51.
38. Hu, X., et al., *Smaller medial temporal lobe volumes in individuals with subjective cognitive decline and biomarker evidence of Alzheimer's disease-Data from three memory clinic studies.* Alzheimers Dement, 2019. **15**(2): p. 185-193.
39. Perrotin, A., et al., *Hippocampal Subfield Volumetry and 3D Surface Mapping in Subjective Cognitive Decline.* J Alzheimers Dis, 2015. **48 Suppl 1**: p. S141-50.
40. Eickhoff, S.B., et al., *A new SPM toolbox for combining probabilistic cytoarchitectonic maps and functional imaging data.* Neuroimage, 2005. **25**(4): p. 1325-35.
41. Grothe, M., H. Heinsen, and S.J. Teipel, *Atrophy of the cholinergic Basal forebrain over the adult age range and in early stages of Alzheimer's disease.* Biol Psychiatry, 2012. **71**(9): p. 805-13.

42. Mesulam, M., *The cholinergic lesion of Alzheimer's disease: pivotal factor or side show?* Learn Mem, 2004. **11**(1): p. 43-9.
43. Mesulam, M.M. and C. Geula, *Nucleus basalis (Ch4) and cortical cholinergic innervation in the human brain: observations based on the distribution of acetylcholinesterase and choline acetyltransferase.* J Comp Neurol, 1988. **275**(2): p. 216-40.
44. Vogel, J.W., et al., *Subjective cognitive decline and beta-amyloid burden predict cognitive change in healthy elderly.* Neurology, 2017. **89**(19): p. 2002-2009.
45. Timmers, T., et al., *Amyloid PET and cognitive decline in cognitively normal individuals: the SCIENCe project.* Neurobiol Aging, 2019. **79**: p. 50-58.
46. Striepens, N., et al., *Interaction effects of subjective memory impairment and ApoE4 genotype on episodic memory and hippocampal volume.* Psychol Med, 2011. **41**(9): p. 1997-2006.
47. Minoshima, S., et al., *Metabolic reduction in the posterior cingulate cortex in very early Alzheimer's disease.* Ann Neurol, 1997. **42**(1): p. 85-94.
48. Minoshima, S., et al., *Discordance between traditional pathologic and energy metabolic changes in very early Alzheimer's disease. Pathophysiological implications.* Ann N Y Acad Sci, 1999. **893**: p. 350-2.
49. Chetelat, G., et al., *Mild cognitive impairment: Can FDG-PET predict who is to rapidly convert to Alzheimer's disease?* Neurology, 2003. **60**(8): p. 1374-7.
50. Drzezga, A., et al., *Cerebral metabolic changes accompanying conversion of mild cognitive impairment into Alzheimer's disease: a PET follow-up study.* Eur J Nucl Med Mol Imaging, 2003. **30**(8): p. 1104-13.
51. Prichep, L.S., et al., *Prediction of longitudinal cognitive decline in normal elderly with subjective complaints using electrophysiological imaging.* Neurobiol Aging, 2006. **27**(3): p. 471-81.
52. van Harten, A.C., et al., *Preclinical AD predicts decline in memory and executive functions in subjective complaints.* Neurology, 2013. **81**(16): p. 1409-16.
53. Peter, J., et al., *Gray matter atrophy pattern in elderly with subjective memory impairment.* Alzheimers Dement, 2014. **10**(1): p. 99-108.
54. van Harten, A.C., et al., *Cerebrospinal fluid Abeta42 is the best predictor of clinical progression in patients with subjective complaints.* Alzheimers Dement, 2013. **9**(5): p. 481-7.
55. Wolfsgruber, S., et al., *Cerebrospinal Fluid Biomarkers and Clinical Progression in Patients with Subjective Cognitive Decline and Mild Cognitive Impairment.* J Alzheimers Dis, 2017. **58**(3): p. 939-950.
56. Kilimann, I., et al., *Parallel Atrophy of Cortex and Basal Forebrain Cholinergic System in Mild Cognitive Impairment.* Cereb Cortex, 2017. **27**(3): p. 1841-1848.
57. Schmitz, T.W., et al., *Longitudinal Alzheimer's Degeneration Reflects the Spatial Topography of Cholinergic Basal Forebrain Projections.* Cell Rep, 2018. **24**(1): p. 38-46.

58. Wolf, D., et al., *Association of basal forebrain volumes and cognition in normal aging.* Neuropsychologia, 2014. **53**: p. 54-63.
59. Grothe, M.J., et al., *Cognitive Correlates of Basal Forebrain Atrophy and Associated Cortical Hypometabolism in Mild Cognitive Impairment.* Cereb Cortex, 2016. **26**(6): p. 2411-2426.
60. Teipel, S.J., et al., *Basal Forebrain Volume, but Not Hippocampal Volume, Is a Predictor of Global Cognitive Decline in Patients With Alzheimer's Disease Treated With Cholinesterase Inhibitors.* Front Neurol, 2018. **9**: p. 642.
61. Zaborszky, L., et al., *Stereotaxic probabilistic maps of the magnocellular cell groups in human basal forebrain.* Neuroimage, 2008. **42**(3): p. 1127-41.

Legends Of The Supplementary Files

Text S1. Neuropsychological Tests

Table S1. Demographic, clinical and neuropsychological characteristic for subgroup of HC and SCD with and without CSF information.

Values are represented with mean ± standard error. Subscripts denote number of missing values. [a] Kruskal-Wallis Non-Parameter Test; [b] Chi-Square Test. [c] ANCOVA Test controlling for age, gender, education and APOE4 status.

Table S2. Demographic, clinical and neuropsychological characteristic for amyloid-stratified HC and SCD subgroups.

Values are represented with mean ± standard error. Subscripts denote number of missing values; HC-, healthy control with amyloid negative (-); HC+, healthy control with amyloid positive (+);SCD-, subjective cognitive decline with amyloid negative (-); SCD+, subjective cognitive decline with amyloid positive (+);[a]Significantly different ($p < 0.05$) between HC+ and HC- ; [b]Significantly ($p < 0.05$) different between SCD+ and SCD-; [c]Significantly different ($p < 0.05$) between HC+ and SCD+; [d]Significantly different ($p < 0.05$) between HC- and SCD-.

Table S3. Interaction effect of amyloid status factor (Aβ+/Aβ-) and group factor (HC, SCD) on BF and the other subnuclei.

Values are represented with estimated marginal mean ± standard error. ns: not significance; Significance levels: * $p < 0.05$; HC-: amyloid negative HC; SCD-: amyloid negative SCD; HC+: amyloid positive HC; SCD+: amyloid positive SCD.

Table S4. Interaction effect of amyloid status factor (Aβ+/Aβ-) and group factor (HC, SCD) on the exploratory structural brain regions.

Values are represented with estimated marginal mean ± standard error. ns: not significance; HIP: Hippocampus; BA: Brodmann area; HC-: amyloid negative HC; SCD-: amyloid negative SCD; HC+: amyloid positive HC; SCD+: amyloid positive SCD.

Table S5. Interaction effect of amyloid status factor (Aβ+/Aβ-) and group factor (HC, MCI) on BF regions.

Values are represented with estimated marginal mean ± standard error. ns: not significance; HIP: Hippocampus; BA: Brodmann area; HC-: amyloid negative HC; MCI-: amyloid negative MCI; HC+: amyloid positive HC; MCI+: amyloid positive MCI.

Table S6. Exploratory analyses according to tau pathology.

Table S7. Exploratory analyses according to both amyloid and tau pathology.

Figures

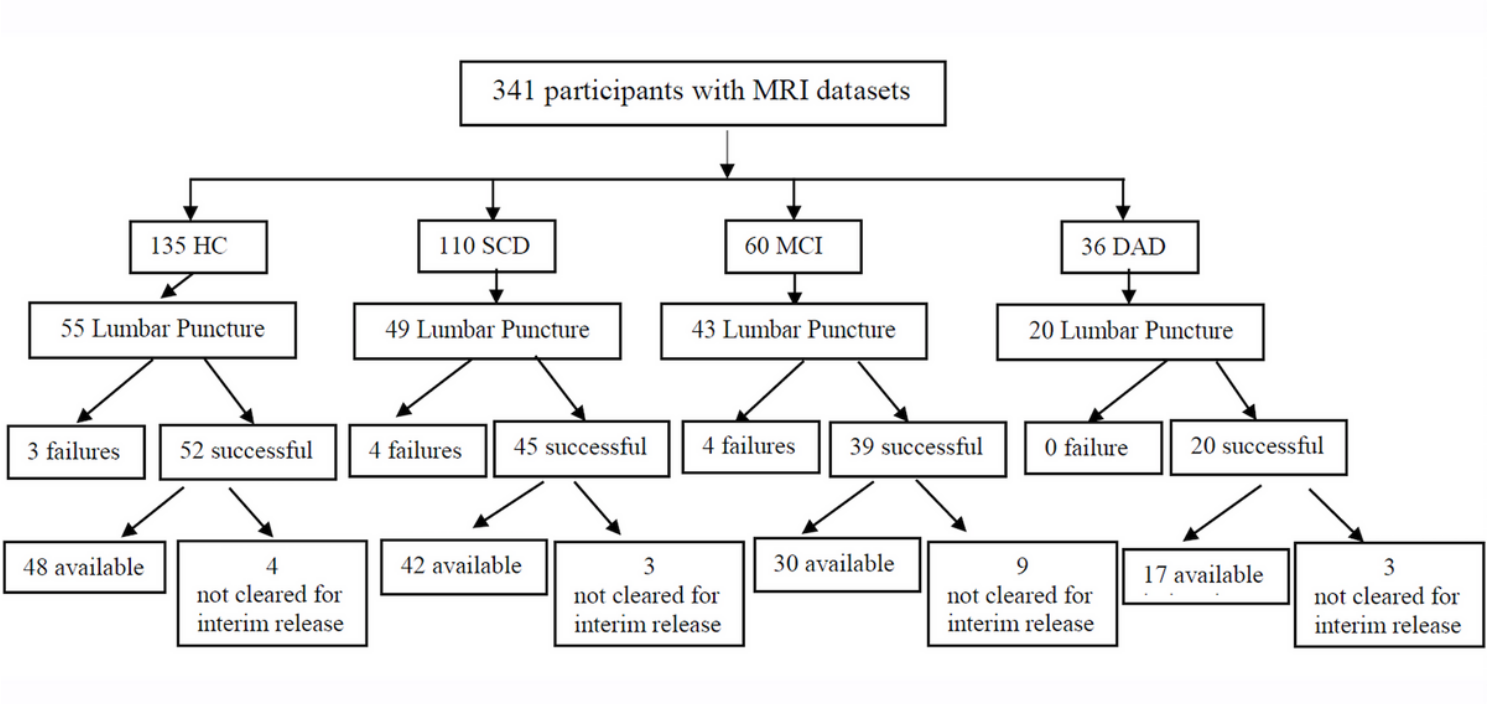

Figure 1

Flow chart of number of participants with lumbar puncture in HC, SCD, MCI and DAD. HC, Healthy Control; SCD, Subjective Cognitive Decline; MCI, Mild Cognitive Decline; DAD, Dementia due to Alzheimer's Type;

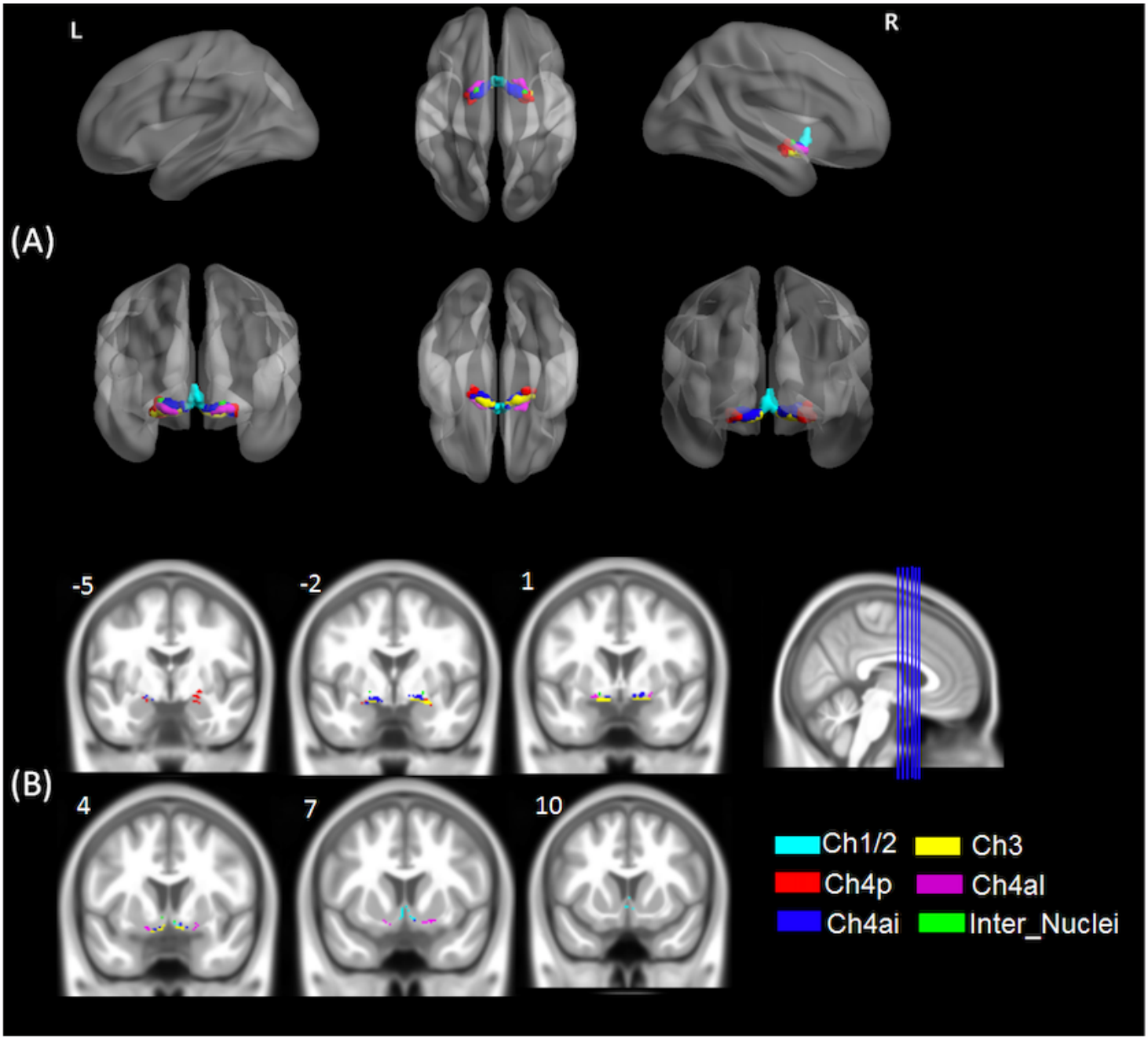

Figure 2

Illustration of the subregions of the cholinergic basal forebrain (BF). (A) 3D view of BF from the sagittal, coronal and axial view: L = left; R=right (B) Superposition of the BF mask on the IXI555 template. The coronal slices range from from Y = -5 to Y = +10 mm (every 3 mm). Abbreviations: Ch1/2: medial septum and the vertical limb of the diagonal band of Broca; Ch3: horizontal limb of the diagonal band of Broca. Nucleus basalis Meynert (Ch4) can be divided into an anterior lateral part (Ch4al), anteriore and intermediate subregions (Ch4ai) and an posterior part (Ch4p). For completeness we also added the interstitial nuclei (Inter_Nuclei) here, but due to its small size, covering only a couple of voxels, it was not included into any volumetric analysis.

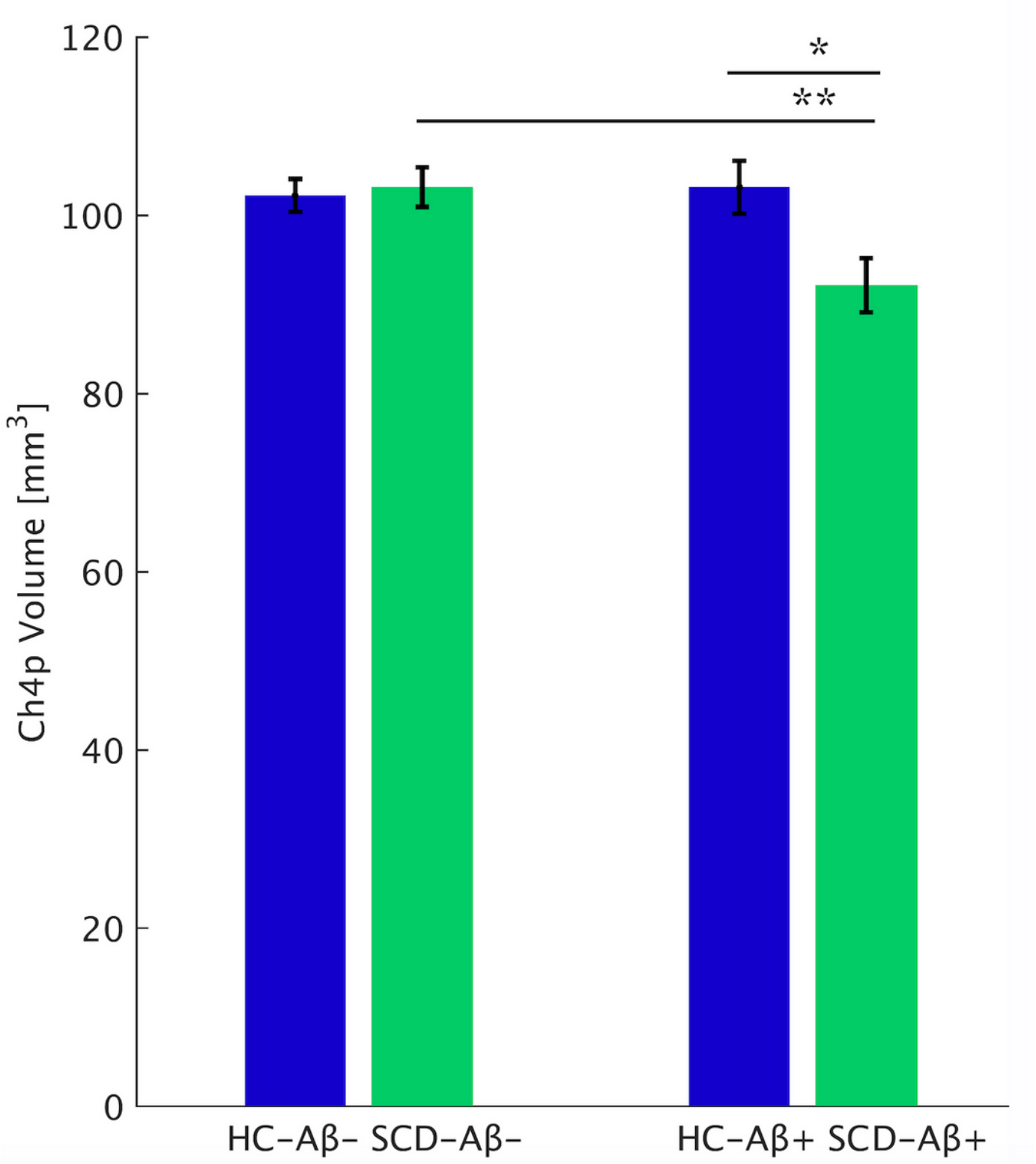

Figure 3

: Interaction effect of amyloid status factor (Aβ+/Aβ-) and group factor (HC, SCD) on Ch4p volume. Displayed are the estimated marginal means of the Ch4p volume. HC-Aβ-: amyloid negative HC; SCD-Aβ-: amyloid negative SCD; HC-Aβ+: amyloid positive HC; SCD-Aβ+: amyloid positive SCD. * Significant post hoc test: HC-Aβ+ vs. SCD-Aβ+; p-value = 0.032. ** Significant post hoc test: SCD-Aβ+ vs. SCD-Aβ-; p-value = 0.006.

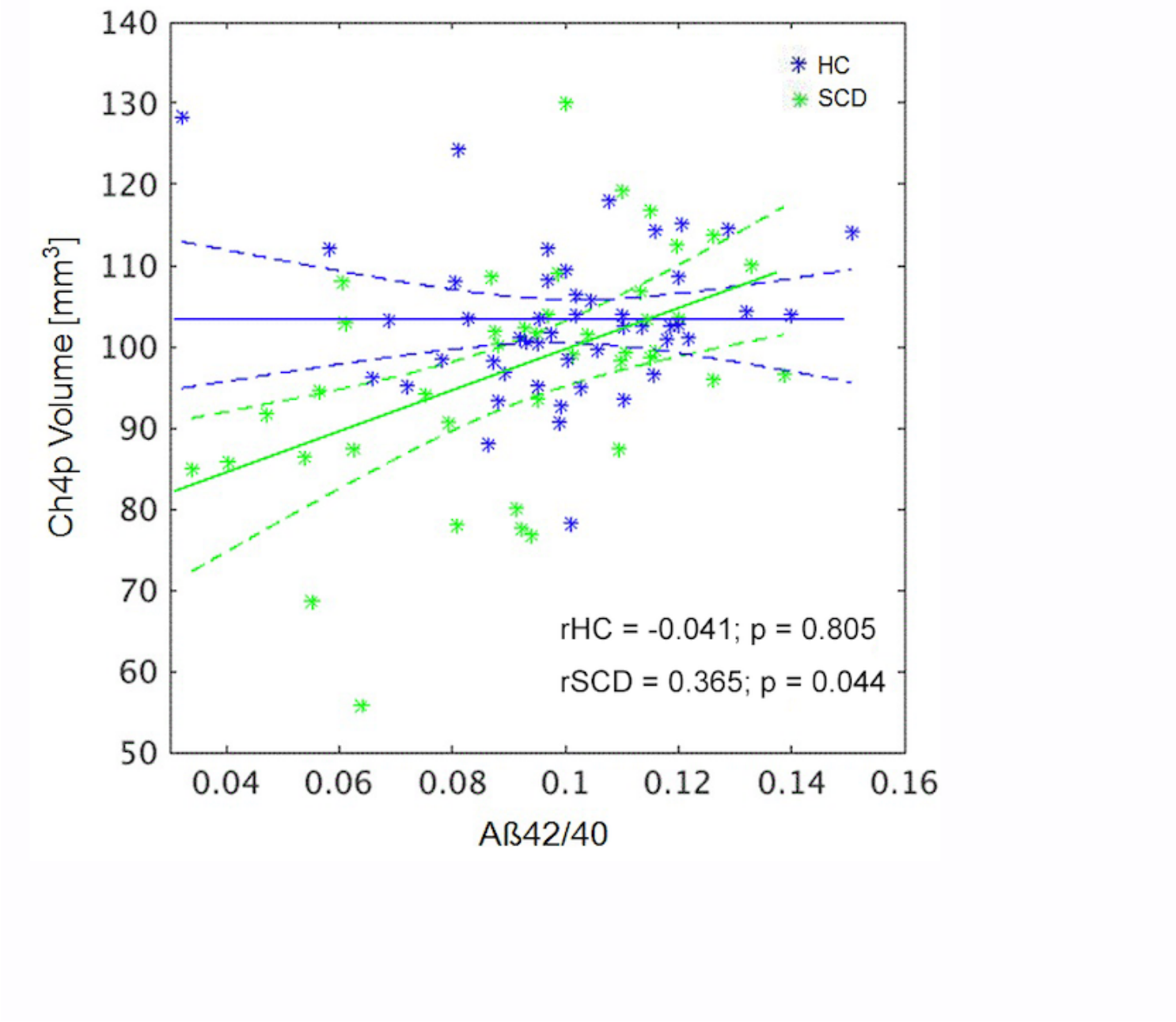

Figure 4

Partial correlations between Ch4p volume and Aβ42/40 ratio in HC and SCD group. The dotted area is the 95% confidential interval. Ch4p volume shown here is after correcting for TIV.

Supplementary Files

This is a list of supplementary files associated with this preprint. Click to download.

- SupplementaryMaterials1152020.docx